Electrical and Thermoelectrical Transport Properties of Dirac Fermions through a Quantum Dot

Tomosuke Aono

Department of Electrical and Electronic Engineering, Ibaraki University, Hitachi 316-8511, Japan

We investigate the conductance and thermopower of massless Dirac fermions through a quantum dot using a pseudogap Anderson model in a noncrossing approximation. When the Fermi level is at the Dirac point, the conductance has a cusp where the thermopower changes its sign. When the Fermi level is away from the Dirac point, the Kondo temperature shows a quantum impurity transition between an asymmetric strong-coupling Kondo state and a localized moment state. The conductance shows a peak near this transition and reaches the unitary limit at low temperatures. The magnitude of the thermopower exceeds k_B/e , and the thermoelectric figure of merit exceeds unity.

KEYWORDS: Dirac fermions, pseudogap Kondo effect, electron transport, thermoelectrics, quantum dot

Electron transport in graphene¹ is currently under active investigation. Graphene-based quantum dot (QD) structures are fabricated and Coulomb blockade peaks are observed.^{2–5} In semiconductor QD systems, it is known that the exchange coupling between a local spin in a QD and conduction electrons induces the Kondo effect.^{6,7} The Kondo effect in graphene has been discussed in connection with the magnetic impurity problem in massless Dirac fermions.^{8–15} A recent experiment shows that the Kondo effect can be induced by lattice vacancies.¹⁶ The Kondo effect probably occurs in another representative Dirac fermions, that is, the surface state of a topological insulator. A single Dirac cone appears on the surfaces of three-dimensional topological insulators.^{17–21} Several theoretical studies on the Kondo effect in this system have been conducted.^{22–26}

The Kondo problem in massless Dirac fermions is an important part of the pseudogap Kondo problem,²⁷ in which the density of states of conduction electrons $\rho(\omega)$ obeys a power law: $\rho(\omega) \propto |\omega|^r$. For example, it is realized in unconventional superconductors.^{27,28} The numerical renormalization group (NRG) calculations^{29,30} and perturbative scaling theory^{31,32} show that the system exhibits an impurity quantum phase transition. For the massless Dirac fermion model, in which r = 1, when the Coulomb interaction is sufficiently strong, there are three fixed points: the local moment (LM) fixed point, the asymmetric strong-coupling (ASC) or frozen impurity fixed point, and the valence fluctuation (VFI) fixed point located in between.^{29,31,32} The Kondo problem in graphene has been studied as a tunable pseudogap Kondo problem, 8,13 where the transition can be controlled by external gate voltages. Recently, the Kondo effect indicated in ref. 16 has been analyzed using a pseudogap Anderson model.³³

In addition to their electrical transport properties, nanostructured materials have been investigated to improve their thermoelectrical properties,³⁴ which also reveal the electronic states in the materials. For instance, the measurement of the thermopower shows the electron-hole asymmetry in a system. The thermopower under the Kondo effect³⁵ has been examined in QD systems theoretically,^{36,37} and its measurement clarifies the formation of the Kondo resonant state.³⁸ Moreover, typical topological insulators^{17–21} have been known as good thermoelectrical materials.

We investigate electrical and thermoelectrical transport properties of Dirac electrons through a QD via tunneling barriers. The barriers exhibit pseudogaps, which result in an impurity quantum phase transition. We discuss this transition in connection with electron transport properties. We also show that thermoelectrical properties are enhanced by a pseudogap. To this end, we study the conductance, the Kondo temperature defined by the impurity magnetic susceptibility, the thermopower, and the figure of merit, using a pseudogap Anderson model in a noncrossing approximation (NCA). ^{39–42}

Model— We consider a system consisting of a QD connected to the lead i (i = L, R) with a single Dirac cone and the chemical potential μ_i . We discuss electron transport through the QD, as shown in the inset of Fig. 1(a). We focus on the zero-bias-voltage limit, $\mu_L \to \mu_R$, setting $\mu_i = 0$. The position of the Dirac point from the Fermi level is denoted by $-\mu_0$.

The Hamiltonian of the lead i is given by a Dirac Hamiltonian:

$$H_0^{(i)} = \int \frac{d^2k}{(2\pi)^2} (\Psi_{ai}^{\dagger}(\boldsymbol{k}), \Psi_{bi}^{\dagger}(\boldsymbol{k})) M(\boldsymbol{k}) \begin{pmatrix} \Psi_{ai}(\boldsymbol{k}) \\ \Psi_{bi}(\boldsymbol{k}) \end{pmatrix}, (1)$$

with $M(\mathbf{k}) = \begin{pmatrix} -\mu_0 \\ \hbar v_F k e^{-i\theta} \end{pmatrix}$, where $\Psi_{ai}(\mathbf{k})$ are the annihilation operators of Dirac fermions, v_F is the Fermi velocity, $\mathbf{k} = (\mathbf{k} \cos \theta, \mathbf{k} \sin \theta)$ with $\mathbf{k} = |\mathbf{k}|$, and θ stands for the azimuthal angle of \mathbf{k} . The indexes a and b refer to (pseudo) spin indexes. For a single-Dirac-cone system, those are the spin indexes $a = \uparrow$ and $b = \downarrow$. For graphene, a = (A, s) and b = (B, s) with the two sublattices A and B, which play the role of a pseudo spin, and the spin index $s = \uparrow$, \downarrow around the K and K' points. 43

The QD has an energy level $E_{\rm g}$ controlled by a gate voltage. The Hamiltonian of the QD is given by

$$H_{\rm d} = \sum_{s=\uparrow,\downarrow} E_{\rm g} d_s^{\dagger} d_s + U n_{\uparrow} n_{\downarrow}, \qquad (2)$$

where d_s is the annihilation operator of an electron with spin s in the QD, $n_s = d_s^{\dagger} d_s$, and U is the Coulomb energy in the QD. The tunneling Hamiltonian is given by $H_T = \sum_{i=L,R,s} \int \frac{d^2k}{(2\pi)^2} (V_i(\boldsymbol{k}) d_s^{\dagger} \Psi_{si}(\boldsymbol{k}) + \text{h.c.})$. For simplicity, we assume $V_i(\boldsymbol{k}) = V$.

It has been shown that the above model reduces to the pseudogap Anderson model after a series of linear transforma-

tions. 8,24,28 In the energy space, H_0 is given by

$$H_0 = \sum_{\stackrel{i=\text{L,R}}{\sigma=+}} \int d\omega \,\omega \,c_{\sigma i}^{\dagger}(\omega)c_{\sigma i}(\omega), \tag{3}$$

where $c_{\sigma i}(\omega)$ is the annihilation operator of an electron in the lead i with the pseudo-spin index σ at the energy ω . The tunneling Hamiltonian H_T is given by

$$H_{\rm T} = \sum_{i,\sigma} \int d\omega \sqrt{\Gamma(\omega)} d_{\sigma}^{\dagger} c_{\sigma i}(\omega) + \text{h.c.},$$
 (4)

where $\Gamma(\omega) = \alpha |\omega + \mu_0|$ with $\alpha = \frac{V^2}{2\pi(\hbar \nu_F)^2}$. 10,24,25 The power law behavior of $\Gamma(\omega)$ is terminated at the band cutoff $D;^{27,29}$ thus, it is convenient to rewrite $\Gamma(\omega)$ in the form²⁹

$$\Gamma(\omega) = \Gamma_0 \left| \frac{\omega + \mu_0}{D} \right|,$$
 (5)

with $\Gamma_0/D = \alpha$.

We treat the infinite U limit of the model, $H = H_{\rm d} + H_{\rm T} + H_0$, which corresponds to the asymmetric pseudogap Anderson model. 29,31,32 We introduce the auxiliary operators, $d_{\sigma} = b^{\dagger}f_{\sigma}$, where b is the boson operator and f_{σ} is the fermion operator. The constraint $b^{\dagger}b + \sum_{\sigma} f_{\sigma}^{\dagger}f_{\sigma} = 1$ should be satisfied. 39,44 Then, we adopt the NCA $^{39-42}$ to calculate the local density of states on the QD and other quantities. To perform numerical calculations, we evaluate Green's functions in the range of $|\omega| \leq 10D$ and introduce the Lorentzian cutoff in $\Gamma(\omega)$, $\Gamma(\omega) \rightarrow \Gamma(\omega) \cdot D^2/(\omega^2 + D^2)$. The convergence of the NCA equations is monitored using the sum rules on the boson and fermion Green's functions, and the sum rule on the total occupation number in the QD. 41 Those relations are satisfied within 0.1%.

The conductance G and the thermopower S are given by $G = e^2 I_0(T)$ and $S = -I_1(T)/[eTI_0(T)]$ with

$$I_n(T) = -2/h \int d\omega \omega^n \frac{\partial f(\omega)}{\partial \omega} \Gamma(\omega) \text{Im} A^r(\omega), \quad (6)$$

where $f(\varepsilon)$ is a Fermi-Dirac function, $f(\omega) = 1/[\exp\left(\frac{\omega}{k_BT}\right) + 1]$, and $A^r(\omega)$ is the retarded Green's function on the QD.^{37,45} The impurity magnetic susceptibility $\chi(\omega)$ is given by $\chi(\omega) = \int_{-\infty}^{\infty} dt e^{i(\omega+i0^+)t} M(t)$, where $M(t) = i\theta(t)\langle [\hat{M}(t), \hat{M}(0)] \rangle$ with $\hat{M} = g\mu_B/2$ ($f_{\uparrow}^{\dagger}f_{\uparrow} - f_{\downarrow}^{\dagger}f_{\downarrow}$). The static susceptibility $\chi = \chi(0)$ is evaluated using the NCA.⁴⁰ We set $g\mu_B = 1$ and $k_B = 1$ below.

Undoped system— Let us first consider G and the dot occupation number n_d when the Fermi level is at the Dirac point: $\mu_0 = 0$. It has been shown that, in this case, the Kondo temperature $T_K = 0.^{8,13,27}$ In Fig. 1(a), G and n_d are plotted as functions of the gate voltage E_g . There is a cusp in G at $E_g = E_g^*$. Near the cusp, G is linear in $|E_g - E_g^*|$, where n_d changes gradually. This means that the system is in the VFI regime. When $|E_g - E_g^*|$ increases further, G decreases monotonically and shows a double-peak structure. In Fig. 1(b), the local density of states on the QD, $\rho_d(\omega) = (-1/\pi) \text{Im} A^r(\omega)$, is plotted. At $E_g = E_g^*$, $\rho_d(\omega)$ shows a singular peak at the Fermi level, $\omega = 0$, which has already been discussed. 13,30,31 In spite of this sharp peak, the pseudogap in $\Gamma(\omega)$ minimizes G.

In Fig. 2, G and the thermopower S are plotted as functions of $(E_g - E_g^*)/T$ at several temperatures. In each figure, the results are similar in shape. This shows that the separation

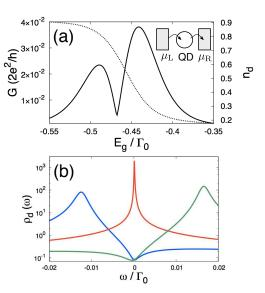


Fig. 1. (Color online) (a) Conductance G (solid line) and occupation number in the QD n_d (dotted line) as functions of gate voltage E_g for $T/\Gamma_0 = 1.0 \times 10^{-2}$ and $D/\Gamma_0 = 10$ ($\alpha = 0.1$). Inset: schematic picture of the QD system. (b) Local densities of states $[\rho_d(\omega)]$ in units of $1/\Gamma_0$ at the left peak (blue), cusp (red), and right peak (green) of G in (a).

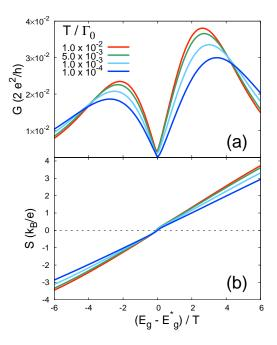


Fig. 2. (Color online) Conductance G (a) and thermopower S (b) for $\mu_0=0$ as functions of normalized gate voltage, $(E_{\rm g}-E_{\rm g}^*)/T$, where $E_{\rm g}^*$ is the gate voltage at the cusp of G.

of the double peaks of G depends linearly on T. In addition, $S \propto (E_g - E_g^*)/T$. This means that E_g^* defines the boundary between electron-like and hole-like transport processes. This is in agreement with the fact that E_g^* is in the VFI regime. Note that the magnitude of S exceeds $k_{\rm B}/e \simeq 86$ [$\mu {\rm V/K}$].

The above results of G and S are explained largely by

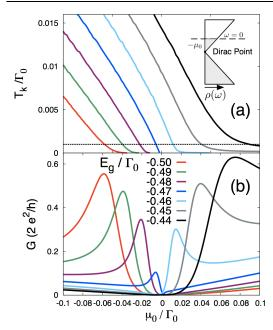


Fig. 3. (Color online) (a) Kondo temperature T_K/Γ_0 vs μ_0 for various gate voltages; T_K is defined by $T_{\rm K}\chi(T_{\rm K})=0.071$. The dotted line indicates $T_{\rm K}/\Gamma_0=1.0\times 10^{-3}$. Inset: schematic picture of density of states in the leads. (b) Conductance G vs μ_0 at $T/\Gamma_0=1.0\times 10^{-3}$.

 $\rho_{\rm d}(\omega)$. When U=0,

$$\rho_d(\omega) = \frac{-1}{\pi} \text{Im} \frac{1}{\omega - E_g + i\Gamma_0 |\omega/D|}.$$
 (7)

To adjust the QD level shift due to U, we replace E_g by $E_g - E_g^*$. When U = 0, the peak width of $\rho_d(\omega)$, $\Gamma_0|\omega/D|$, is smaller than T, since $D/\Gamma_0 > 1$ and $T/\Gamma_0 \ll 1$. This is valid for the present model. Then, $\rho_d(\omega)$ can be approximated using a Dirac delta function inside the integral of eq. (6); $\rho_d(\omega) \sim \delta(\omega - (E_g - E_g^*))$. This explains the linear dependence of G near the cusp, and the peak separation of G is proportional to G. Similarly, G in eq. (6) is proportional to G in G in

Doped system— Next, we consider the case where the Fermi level ($\omega=0$) is away from the Dirac point, $\mu_0 \neq 0$, as depicted in the inset of Fig. 3(a). In this case, a clear sign of the transition between the ASC and LM states appears with the tuning of the external voltages.^{8,13} We focus on the transition induced by μ_0 . In general, μ_0 determines the renormalization of the dot level, and the position of the renormalized level controls the transition.

In Fig. 3(a), the Kondo temperature $T_{\rm K}$ is plotted as a function of μ_0 for several $E_{\rm g}$ values, where $T_{\rm K}$ in this paper is defined in terms of χ by $T_{\rm K}\chi(T_{\rm K})=0.0701.^{46,47}$ There is an asymmetry with respect to the sign of μ_0 . In particular, $T_{\rm K}$ vanishes at $\mu_0=\mu_0^*$ when $\mu_0^*<0$; $T_{\rm K}=0$ indicates the LM phase. When $E_{\rm g}$ approaches $E_{\rm g}^*$, where $E_{\rm g}^*/\Gamma_0\simeq-0.468$ in Fig. 2, μ_0^* goes to zero. This asymmetry has been reported in ref. 13 for the critical Kondo coupling model, $E_{\rm g}=E_{\rm g}^*$. A linear dependence of $T_{\rm K}$ is found in all curves. It is seen most clearly in the curve of $E_{\rm g}/\Gamma_0=-0.47$ (blue line). This coincides with the previous results. 8,13,27 The linear coefficient is

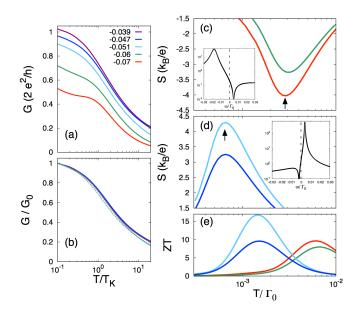


Fig. 4. (Color online) (a) Conductance G vs $T/T_{\rm K}$ at $E_{\rm g}/\Gamma_0 = -0.5$ for various μ_0/Γ_0 values. (b) Normalized conductance G/G_0 vs $T/T_{\rm K}$ with $G_0 = G(0.1T_{\rm k})$ for three uppermost curves in (a), and $(E_{\rm g}/\Gamma_0, \mu_0/\Gamma_0) = (-0.48, -0.015)$ (dotted red line) and $(-0.47, -1.75 \times 10^{-3})$ (dotted green line). (c,d,e) Temperature dependences of S (c,d) and figure of merit ZT (e) for $(E_{\rm g}/\Gamma_0, \mu_0/\Gamma_0) = (-0.5, -0.005)$ (red), (-0.5, -0.01)(green), (-0.46, 0.002)(light blue), and (-0.46, 0.004)(blue). Insets: (c,d) local densities of states $[\rho_d(\omega)]$ in units of $1/\Gamma_0$ at the points indicated by the arrows.

about 0.368 for $E_{\rm g}=E_{\rm g}^*,^{13,27}$ while here it is about 0.33 in the vicinity of $E_{\rm g}^*$. There are deviations from linearity when $T_{\rm K}$ approaches zero and when $E_{\rm g}$ is away from $E_{\rm g}^*$. We find that the linear coefficient weakly depends on $E_{\rm g}$.

The behavior of $T_{\rm K}$ correlates with G. Figure 3(b) shows G as a function of μ_0 for $T/\Gamma_0=1.0\times 10^{-3}$. It has a peak structure; at the peak, $T\simeq T_{\rm K}$, as indicated in (a) by the intersection of each curve with the dotted line. When $T_{\rm K}=0$, where the system is the LM regime, G is small. As μ_0 decreases, $T_{\rm K}$ increases when $\mu_0<\mu_0^*$. This results in an increase in G since $T_{\rm K}/T$ increases. When μ_0 further decreases, G starts to decrease. This indicates that the system enters the VFI regime as in a conventional QD since μ_0 controls the effective dot level. (This point will be further discussed below.)

Now, we discuss the temperature dependence of G. Figure 4(a) shows G as a function of T/T_K for several μ_0 values at $E_g/\Gamma_0 = -0.5$. All the curves show that G increases as T decreases. When μ_0 approaches μ_0^* , G reaches the unitary limit. In graphene QD systems, the Coulomb blockade peak heights are about $0.1e^2/h$ because of the pseudogap.²⁻⁵ Thus, this increase in G may provide direct evidence of the Kondo effect in a graphene QD. When μ_0 decreases, G(T) shows a hump. This feature appears in the VFI regime in the conventional QD system. 48,49 This means that the crossover from the ASC state to the VFI state appears when μ_0 changes. This is consistent with the peak structure of G in Fig. 3(b). Finally, we comment on the universality of G within the NCA. In Fig. 4(b), $G/G(T = 0.1T_K)$ is plotted as a function of T/T_K in the vicinity of the transition point, for five different values of μ_0 and E_{g} . These curves collapse to a universal curve.

Now, we discuss the thermoelectrical properties in the vicinity of $\mu_0 = 0$, where $G \simeq 0$. Figures 4(c) and 4(d) show

the curves of S plotted as a function of T in the LM (c) and the VFI (d) regimes, respectively. In both cases, $|S| > k_B/e$; S has a negative sign for LM and a positive sign for VFI. The insets show $\rho_d(\omega)$ at the peaks of S as indicated by the arrows. In those figures, a sharp peak and a dip appear on opposite sides of the Fermi level ($\omega = 0$); the dip originates from the pseudogap and the peak from the renormalized localized level. This asymmetry of $\rho_d(\omega)$ leads to the increase in |S| since I_1 in eq. (6) is the "moment" of $\rho_d(\omega)\Gamma(\omega)$. We emphasize that the presence of the pseudogap is essential to the increase since both the sharp peak and the dip originate from the pseudogap.

The increase in |S| indicates that the QD system can be a good thermoelectrical device, which is characterized by the figure of merit, $ZT = S^2GT/\kappa$, ³⁴ where κ is the thermal conductivity, given by $\kappa = [I_2(T) - I_1(T)^2 / I_0(T)] / T^{.37,45}$ The reason for this is as follows. Since thermal transport is determined by electron transport, κ is expected to be on the order of TG. [The Wiedemann-Franz law, $\kappa/(TG) = \pi^2/3(k_B/e)^2$ is not satisfied since the system is not in the Fermi liquid regime.] This means that ZT can be increased by S. When ZT > 1, the system is regarded as a good thermoelectrical material. Recent studies^{17–21} showed that a single Dirac cone appears on the surfaces of Bi₂Te₃, Bi₂Se₃, and Sb₂Te₃. Those materials are also known as good thermoelectrical materials. Figure 4(e) shows ZT as a function of T in the LM and VFI regimes. This figure also shows that ZT > 1 is achieved when $|S| > k_{\rm B}/e$; moreover, $ZT \gtrsim 10$ in a certain range. The results show that the increase in ZT correlates with the increase in |S| as explained above. Our results are also consistent with the theory on the optimization of ZT by Mahan and Sofo,⁵⁰ where a narrow peak distribution of conduction electrons increases ZT. In the present case, the pseudogap induces the narrow peak as shown in the insets of Figs. 4(c) and (d).

In summary, we have investigated electrical and thermoelectrical properties of the pseudogap Anderson model. In the undoped case, the conductance is much less than $2e^2/h$, whereas the magnitude of the thermopower exceeds $k_{\rm B}/e$. In the doped case, the conductance shows a peak structure, which indicates the transition between the ASC and LM phases, characterized by the Kondo temperature. The unitary limit of the conductance appears at low temperatures. When the magnitude of the thermopower exceeds $k_{\rm B}/e$, the figure of merit is greater than unity. The QD system in Dirac fermions therefore displays two distinctive features induced by the pseudogap, an impurity quantum phase transition, and excellent thermoelectrical properties.

Acknowledgments The author thanks Y. Avishai, A. Golub, T. Nakanishi, and Y. Takane for fruitful discussion and comments on various aspects. The author also acknowledges the support from JSPS and JST.

- A. H. Castro Neto, F. Guinea, N. M. R. Peres, K. S. Novoselov, and A. K. Geim: Rev. Mod. Phys. 81 (2009) 109.
- C. Stampfer, J. Güttinger, F. Molitor, D. Graf, T. Ihn, and K. Ensslin: App. Phys. Lett. 92 (2008) 012102.
- L. A. Ponomarenko, F. Schedin, M. I. Katsnelson, R. Yang, E. W. Hill, K. S. Novoselov, and A. K. Geim: Science 320 (2008) 356.
- S. Moriyama, D. Tsuya, E. Watanabe, S. Uji, M. Shimizu, T. Mori, T. Yamaguchi, and K. Ishibashi: Nano Lett. 9 (2009) 2891.
- J. Güttinger, T. Frey, C. Stampfer, T. Ihn, and K. Ensslin: Phys. Rev. Lett. 105 (2010) 116801.
- 6) D. Goldhaber-Gordon, H. Shtrikman, D. Mahalu, D. Abusch-Magder,

- U. Meirav, and M. A. Kastner: Nature 391 (1998) 156.
- S. M. Cronenwett, T. H. Oosterkamp, and L. P. Kouwenhoven: Science 281 (1998) 540.
- 8) K. Sengupta and G. Baskaran: Phys. Rev. B 77 (2008) 045417.
- B. Uchoa, L. Yang, S. W. Tsai, N. M. R. Peres, and A. H. Castro Neto: Phys. Rev. Lett. 103 (2009) 206804.
- P. S. Cornaglia, G. Usaj, and C. A. Balseiro: Phys. Rev. Lett. 102 (2009) 046801.
- H.-B. Zhuang, Q.-f. Sun, and X. C. Xie: Europhys. Lett. 86 (2009) 58004.
- T. O. Wehling, A. V. Balatsky, M. I. Katsnelson, A. I. Lichtenstein, and A. Rosch: Phys. Rev. B 81 (2010) 115427.
- 13) M. Vojta, L. Fritz, and R. Bulla: Europhys. Lett. 90 (2010) 27006.
- B. Uchoa, T. G. Rappoport, and A. H. Castro Neto: Phys. Rev. Lett. 106 (2011) 016801; 106 (2011) 159901(E).
- 15) L. Fritz and M. Vojta: Rep. Prog. Phys. 76 (2013) 032501.
- J.-H. Chen, L. Li, W. G. Cullen, E. D. Williams, and M. S. Fuhrer: Nat. Phys. 7 (2011) 535.
- Y. Xia, D. Qian, D. Hsieh, L. Wray, A. Pal, H. Lin, A. Bansil, D. Grauer,
 Y. S. Hor, R. J. Cava, and M. Z. Hasan: Nat. Phys. 5 (2009) 398.
- 18) D. Hsieh, Y. Xia, D. Qian, L. Wray, J. H. Dil, F. Meier, J. Osterwalder, L. Patthey, J. G. Checkelsky, N. P. Ong, A. V. Fedorov, H. Lin, A. Bansil, D. Grauer, Y. S. Hor, R. J. Cava, and M. Z. Hasan: Nature 460 (2009) 1101.
- 19) D. Hsieh, Y. Xia, D. Qian, L. Wray, F. Meier, J. H. Dil, J. Osterwalder, L. Patthey, A. V. Fedorov, H. Lin, A. Bansil, D. Grauer, Y. S. Hor, R. J. Cava, and M. Z. Hasan: Phys. Rev. Lett. 103 (2009) 146401.
- 20) Y. L. Chen, J. G. Analytis, J.-H. Chu, Z. K. Liu, S.-K. Mo, X. L. Qi, H. J. Zhang, D. H. Lu, X. Dai, Z. Fang, S. C. Zhang, I. R. Fisher, Z. Hussain, and Z.-X. Shen: Science 325 (2009) 178.
- H. Zhang, C.-X. Liu, X.-L. Qi, X. Dai, Z. Fang, and S.-C. Zhang: Nat. Phys. 5 (2009) 438.
- Q. Liu, C.-X. Liu, C. Xu, X.-L. Qi, and S.-C. Zhang: Phys. Rev. Lett. 102 (2009) 156603.
- 23) M.-T. Tran and K.-S. Kim: Phys. Rev. B 82 (2010) 155142.
- 24) R. Žitko: Phys. Rev. B 81 (2010) 241414.
- X.-Y. Feng, W.-Q. Chen, J.-H. Gao, Q.-H. Wang, and F.-C. Zhang: Phys. Rev. B 81 (2010) 235411.
- A. K. Mitchell, D. Schuricht, M. Vojta, and L. Fritz: Phys. Rev. B 87 (2013) 075430.
- 27) D. Withoff and E. Fradkin: Phys. Rev. Lett. 64 (1990) 1835.
- C. R. Cassanello and E. Fradkin: Phys. Rev. B 53 (1996) 15079; 56 (1997) 11246.
- C. Gonzalez-Buxton and K. Ingersent: Phys. Rev. B 54 (1996) R15614;
 57 (1998) 14254.
- R. Bulla, Th. Pruschke, and A. C. Hewson: J. Phys. Condens. Matter 9 (1997) 10463.
- 31) L. Fritz and M. Vojta: Phys. Rev. B 70 (2004) 214427.
- 32) M. Vojta and L. Fritz: Phys. Rev. B 70 (2004) 094502.
- T. Kanao, H. Matsuura, and M. Ogata: J. Phys. Soc. Jpn. 81 (2012) 063709.
- 34) Y. Dubi and M. Di Ventra: Rev. Mod. Phys. 83 (2011) 131.
- 35) J. Kondo: Prog. Theor. Phys. 34 (1965) 372.
- 36) D. Boese and R. Fazio: Europhys. Lett. **56** (2001) 576.
- 37) B. Dong and X. L. Lei: J. Phys. Condens. Matter 14 (2002) 11747.
- R. Scheibner, H. Buhmann, D. Reuter, M. N. Kiselev, and L. W. Molenkamp: Phys. Rev. Lett. 95 (2005) 176602.
- 39) P. Coleman: Phys. Rev. B 29 (1984) 3035.
- 40) N. E. Bickers: Rev. Mod. Phys. 59 (1987) 845.
- 41) N. S. Wingreen and Y. Meir: Phys. Rev. B 49 (1994) 11040.
- 42) M. Vojta: Phys. Rev. Lett. 87 (2001) 097202.
- 43) For the K' point, the off-diagonal elements of M are replaced by their complex conjugates.
- 44) S. E. Barnes: J. Phys. F 6 (1976) 1375; 7 (1977) 2637.
- 45) J. Liu, Q.-f. Sun, and X. C. Xie: Phys. Rev. B 81 (2010) 245323.
- H. R. Krishna-murthy, J. W. Wilkins, and K. G. Wilson: Phys. Rev. B 21 (1980) 1003.
- 47) L. G. G. V. Dias da Silva, N. Sandler, P. Simon, K. Ingersent, and S. E. Ulloa: Phys. Rev. Lett. 102 (2009) 166806.
- D. Goldhaber-Gordon, J. Göres, M. A. Kastner, H. Shtrikman, D. Mahalu, and U. Meirav: Phys. Rev. Lett. 81 (1998) 5225.
- 49) H. Schoeller and J. König: Phys. Rev. Lett. 84 (2000) 3686.
- 50) G. D. Mahan and J. O. Sofo: Proc. Natl. Acad. Sci. U. S. A. 93 (1996)

7436.